Available online at www.sciencedirect.com

ScienceDirect

Geochimica et Cosmochimica Acta 311 (2021) 316–331

Geochimica et Cosmochimica Acta

www.elsevier.com/locate/gca

Carbon isotopic composition of plant waxes, bulk organics and carbonates from soils of the Serengeti grasslands

Daolai Zhang [a,1], Emily J. Beverly [b,2], Naomi E. Levin [b], Efrain Vidal [a], Yannick Matia [a], Sarah J. Feakins [a,*]

[a] Department of Earth Sciences, University of Southern California, Los Angeles, CA, USA
[b] Department of Earth and Environmental Sciences, University of Michigan, MI, USA

Received 19 January 2021; accepted in revised form 2 July 2021; available online 6 July 2021

Abstract

The carbon isotopic composition of different carbon-bearing materials, organic and inorganic, is commonly used to reconstruct distributions of tropical C_4 grasslands. However, no study of modern soils has yet combined carbon isotopic compositions ($\delta^{13}C$) of bulk soil organic matter (SOM), soil carbonate (SC), plant wax *n*-alkanes (alk) and *n*-alkanoic acids (acid) to allow for comparison between all four materials. Here, we studied carbonate-precipitating, grassland soils across the Serengeti ecosystem, Tanzania to directly compare $\delta^{13}C$ values of these four materials using samples from 11 sites along a NW–SE transect and depth profiles at each location. Among the soil carbonates found at 9 sites, the $\delta^{13}C$ results ($\delta^{13}C_{SC}$ mean = 0.5 ‰, $1\sigma = 0.8$‰, $n = 70$ nodules collected), denote C_4 grasses exclusively, but soil carbonates are absent from two of the three sites with trees. Organics were measured at all 11 sites including bulk ($\delta^{13}C_{SOM}$ −13.1 ± 1.8‰) and plant wax biomarkers (e.g., $\delta^{13}C_{29alk}$ −23.5 ± 3.1, $\delta^{13}C_{31alk}$ −22.2 ± 2.0, $\delta^{13}C_{33alk}$ −21.9 ± 1.8, $\delta^{13}C_{28acid}$ −19.1 ± 2.1‰, $\delta^{13}C_{30acid}$ −21.1 ± 2.6‰, and $\delta^{13}C_{32acid}$ −20.1 ± 1.7‰). $\delta^{13}C$ values in organic materials record the dominance of C_4 grasses at the sampled sites. Surface samples are more negative than those at depth at most sites, reflecting changes in atmospheric composition and surficial inputs in recent decades, and degradation at depth over centuries. We found significant correlations between each of the organic proxies, but the $\delta^{13}C_{29alk}$ is overly responsive to tree inputs (greater C_{29} concentration and ^{13}C-depletion relative to other homologues), whereas the $\delta^{13}C_{31alk}$, $\delta^{13}C_{33alk}$ and $\delta^{13}C_{32acid}$ are robust recorders of vegetation cover. Of all materials considered (plant wax, SOM and soil carbonates), plant wax *n*-alkanes and *n*-alkanoic acids have the broadest applicability, extending to non-carbonate bearing soils, and to lacustrine and marine sedimentary archives.

Keywords: Carbon isotopes; Leaf wax; Soil carbonates; Grassland; Serengeti

1. INTRODUCTION

Carbon isotope geochemistry has been key to reconstructing the Neogene emergence of extensive tropical grasslands (Quade et al., 1989; Ehleringer et al. 1991). While all plants use the Calvin-Benson (C_3) carbon fixation pathway, tropical grasses also use the Hatch-Slack (C_4) pathway with clear distinction in their carbon isotopic composition (Cerling, 2014). A range of carbon-bearing materials record the prevalence of these vegetation types,

* Corresponding author.
E-mail address: feakins@usc.edu (S.J. Feakins).
[1] Permanent address: Qingdao Institute of Marine Geology, Qingdao, China.
[2] Permanent address: Department of Earth and Atmospheric Sciences, University of Houston, TX, USA.

https://doi.org/10.1016/j.gca.2021.07.005
0016-7037/

including carbonates, bulk organic matter and plant wax biomarkers. Comparison of carbon isotope proxies finds corroborating evidence for C_4 expansion (Freeman and Colarusso, 2001; Feakins et al., 2013; Uno et al., 2016a; Feakins et al., 2020; Sarangi et al., 2021), but differences in how carbon-bearing materials record this expansion merits further investigation.

While soil carbonates have been frequently sampled in rift valley outcrops in eastern Africa, the nodules are slow-forming (500–1000 years; Targulian and Krasilnikov, 2007) and their use in environmental reconstructions is limited to climates, lithologies and pedogenic facies where soil carbonates form (Levin et al., 2004; Wynn 2004). Bulk organic approaches offer the potential to extend beyond carbonate-forming soils to all soils, as in extensive modern calibrations (Cerling et al., 2011); however, degradation may limit the timespan and fidelity of the proxy (Wynn, 2007). Within bulk organics, compound specific approaches can untangle heterogeneous organic inputs to isolate plant-derived biomarkers (Magill et al., 2013), but a knowledge gap remains as to the archiving of plant wax signals in soils and sediments (Diefendorf and Freimuth, 2017). An emerging view is that the persistence of soil organics (whether bulk or biomarker) is not as much a function of molecular stability, as it is an ecosystem property (Schmidt et al., 2011). Thus, it is important to study soils in a range of ecosystems, in both surface soils and in profiles of mineral soils bearing older and altered organic components. Soils are useful targets for proxy calibration studies as they characterize an integrated record of vegetation and taphonomic processes (Schwab et al., 2015) and contain stocks of plant wax greater than that of living plants (Wu et al., 2019) that can be compared to sediments eroded by rivers (Feakins et al, 2018) or wind (Schefuss et al., 2003; Rommerskirchen et al., 2003) and deposited in lacustrine (Garcin et al., 2014) or marine sediments (Rommerskirchen et al., 2006a). Further, carbonate-bearing soils allow for the direct comparison of *in situ* plant wax, soil organic and soil carbonate proxies.

In this study, we surveyed a NW–SE transect across the carbonate-precipitating soils of the Serengeti, an extensive grassland-dominated ecosystem in eastern Africa. We measured the carbon isotopic composition of soil carbonate nodules and clast coatings, soil organic matter, as well as plant wax *n*-alkanes and *n*-alkanoic acids, in order to compare these widely used methods within the same soil profiles. This comparison is important to support integration of available proxies when reconstructing past vegetation change, especially between settings where not all materials are available. The location of this study in eastern Africa is of direct relevance to efforts to reconstruct the past extent of tropical C_4 grasslands, including habitats associated with hominin fossil sites.

2. MATERIALS AND METHODS

2.1. Study sites

The Serengeti ecosystem spans 30,000 km^2 of grassland plains, riverine forest and woodlands, straddling the Tanzania-Kenya border in eastern Africa between 34 and 36°E longitude, and 1–2°S (Fig. 1; Reed et al., 2009). At our study sites, mean annual temperatures vary from 19.2 to 22.8 °C and mean annual precipitation varying from 449 to 846 mm (Table 1; Fick and Hijmans, 2017). Elevation ranges from 1153 to 1667 m above sea level. There are two rainy seasons: March to May, and October to November (Norton-Griffiths et al., 1975).

Vegetation classifications for the Serengeti ecosystem were available from a previous survey of vegetation based on Landsat remote sensing and ground-truthing in 1998–2002 (Reed et al., 2009). The vegetation classifications were identified for the study sites in this transect (Table 1) and correspond to observed conditions in 2018. Most sites are grasslands (<10% woody cover), except for three sites (Banagi, Kemarishe and Makoma; 20–50% tree canopy cover). At Banagi, Kemarishe and Makoma the complete vegetation classifications were closed treed shrubland, mixed open grassland to woodland and open grassed woodland respectively. These classifications indicate that trees contribute secondarily (i.e. <50%) to the shrub canopy closure (80–100%) at Banagi. Trees also form 20 to 50% canopy cover in open grasslands/woodlands at Kemarishe and Makoma.

2.2. Field methods

During February 2018, we collected 26 soil samples from 11 sites distributed along a NW-SE longitude transect across Serengeti ecosystem, Tanzania, from 34.5°E to 35°E (Fig. 1). The location and altitude of each site was recorded by a handheld GPS unit with an error of ±10 m on the horizontal location. For each site, soil pits were dug till refusal (up to 160 cm). Indurated petrocalcic horizons limited further digging in some locations. Carbonate nodules and coatings were sampled at sites where found (all sites except Kemarishe and Makoma) for carbon isotopic analyses considered in this study, as well as in a companion study of triple oxygen isotopes and clumped isotopes (Beverly et al., 2021). Samples were collected for analysis of organic contents from the upper soil in the top 10 cm of soil below the litter layer, mid-depth samples were collected at around 60 cm and deep samples were collected at around 100–160 cm. Mid and deep samples were collected near to the top and the bottom of where soil carbonates were found. Samples at each locality and depth horizon were made up of three sub-samples randomly taken within the 1.5 m width of the soil pit, using a metal scoop. Samples were sealed in bags on site; after one month in transit, they were frozen upon arrival at the laboratory.

2.3. Laboratory methods

2.3.1. Lipid extraction and compound identification

Soil samples were freeze-dried, powdered and extracted two times with 9:1 v/v dichloromethane (DCM) to methanol (MeOH) by an Accelerated Solvent Extractor (ASE 350, Dionex), at 100 °C and 1500 psi. Total lipid extracts (TLE) from soils were then separated into neutral (containing *n*-alkanes) and acid (containing *n*-alkanoic acids) frac-

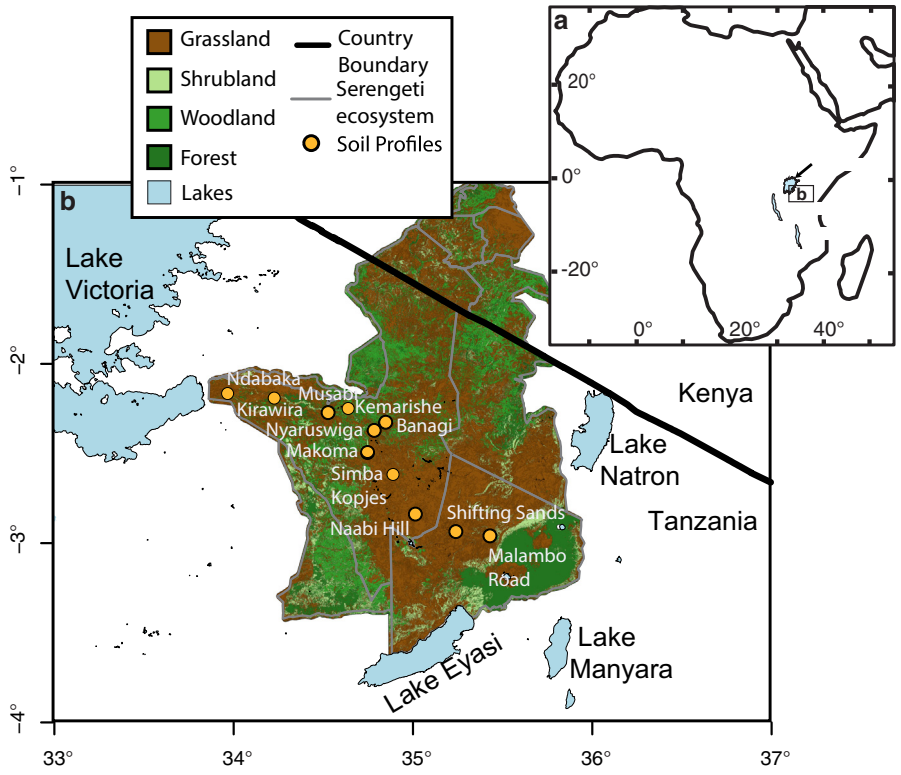

Fig. 1. (a) Location of the Serengeti ecosystem within Africa. (b) Map of study region showing the Serengeti ecosystem spanning Tanzania and Kenya, the soil sampling locations (yellow points) along a transect within the Ngorongoro Conservation Area and Serengeti National Parks in Tanzania. Vegetation map simplified from Reed et al. (2009) to show only grassland, shrubland, woodland, and forest vegetation. (For interpretation of the references to color in this figure legend, the reader is referred to the web version of this article.)

tions by column chromatography through LC-NH_2 gel, eluted by 2:1 v/v DCM to isopropanol and 4% formic acid in diethyl ether respectively. The *n*-alkanes were purified from the neutral fraction through silica gel by hexane. The acid fraction was methylated using methanol of known isotopic composition, in a mixture of 95% methanol, 5% HCl v/v, at 70 °C overnight. Water was added and the *n*-alkanoic acid methyl esters (FAMEs) was separated by liquid:liquid extraction from aqueous solution. The methylated product was dried by passing through anhydrous sodium sulfate columns and further purified by passing through a silica gel column chromatography, eluting with hexane and DCM to collect the FAMEs.

Both fractions of the *n*-alkanes and *n*-alkanoic acids were identified using gas chromatography (Agilent 6890) coupled with mass-selective detector (Agilent 5973). For quantification, the response on the flame ionization detector for *n*-alkanes and *n*-alkanoic acid methyl esters were converted to mass via calibration daily with in-house standard mixtures of the same compounds of known and varied concentrations to define a response factor separately for the four *n*-alkane homologues and three *n*-alkanoic acid methyl ester homologues. Calibration uncertainty (precision) is better than 2% based upon replicate measurements of the standard.

We report data for the C_{23} to C_{35} *n*-alkanes and the C_{16} to C_{34} *n*-alkanoic acids. Summed concentrations were calculated for each compound class, Σalk and Σacid in μg/g dry sediment and Λalk and Λacid in mg/g OC, for the C_{23} to C_{35} *n*-alkanes and the C_{22} to C_{34} *n*-alkanoic acids. We report standard measures of carbon preference index (CPI) and average chain length (ACL) following the general formulae:

$$CPI = 2[C_n]/[C_{n-1}] + [C_{n+1}] \quad (1)$$

$$ACL = \Sigma(n * C_n)/\Sigma[C_n] \quad (2)$$

where the chain length (*n*) refers to the C_{23} to C_{35} *n*-alkanes and C_{22} to C_{34} *n*-alkanoic acids.

2.3.2. Compound-specific isotopic analysis

The carbon isotopic compositions of individual compounds were analyzed by gas chromatography-isotopic ratio mass spectrometry (GC-IRMS) using a Thermo Fisher Scientific Trace GC connected to a Delta V Plus IRMS, via an Isolink combustion furnace at 1000 °C. The linearity in isotopic determination for the CO_2 reference pulse was determined daily across a range of peak amplitudes (1–10 V), with a standard deviation of 0.10‰, representing the precision of reference gas measurements. Isotopic abundances were determined relative to a reference gas and calibrated with A6 Mix standard supplied by A. Schimmelmann, Indiana University, with $\delta^{13}C$ values ranging from −33.3 to −28.6‰ on the Vienna Pee Dee Belemnite (VPDB) isotopic scale. The RMS error determined by replicate measurements of the external standard across

Table 1
Site location and characteristics.

Site	Latitude	Longitude[a]	Elevation (masl)[b]	Vegetation[c]	Soil Order[d]	MAT (°C)[e]	MTWQ (°C)[e]	MAP (mm/yr)[e]	PET (mm/yr)[f]	AI[f]	WD (mm/yr)[f]
Malambo Road	−2.9603	35.4364	1354	Dense grassland	Inceptisol	20.9	22.0	499	1583	0.33	1084
Shifting Sands	−2.9355	35.2473	1549	Dense shrubbed grassland	Inceptisol	19.8	20.9	558	1521	0.38	963
Naabi Hill	−2.8396	35.0205	1677	Closed shrubbed grassland	Mollisol	19.2	20.1	734	1486	0.52	752
Simba Kopjes	−2.6169	34.8966	1637	Dense to closed grassland	Mollisol	19.6	20.5	805	1521	0.54	716
Makoma	−2.4930	34.7544	1549	Closed treed shrubland	Inceptisol	20.2	21.0	829	1560	0.55	731
Nyaruswiga	−2.3496	34.8263	1451	Open treed grassland to closed grassland	Mollisol	20.8	21.6	832	1613	0.51	781
Banagi	−2.3290	34.8478	1425	Mixed open grassland to woodland	Inceptisol	20.9	21.8	819	1622	0.51	803
Kemarishe	−2.2498	34.6448	1315	Open grassed woodland	Alfisol	21.6	22.3	834	1659	0.51	825
Musabi	−2.2719	34.5339	1278	Closed grassland	Mollisol	21.9	22.5	830	1659	0.51	829
Kirawira	−2.1883	34.2322	1215	Dense to closed grassland	Mollisol	22.4	22.9	838	1655	0.53	817
Ndabaka	−2.1654	33.9734	1153	Dense to closed grassland	Vertic Mollisol	22.8	23.2	846	1642	0.55	796

[a] datum WGS 1984.
[b] meters above sea level.
[c] vegetation from Reed et al. (2009).
[d] Soil Order identified based on field observations and climate, to provide a general understanding of soil type, but is not intended to be an absolute USDA soil classification.
[e] MAT = Mean Annual Temperature, MTWQ = Mean Temperature Warmest Quarter, MAP = Mean Annual Precipitation from Fick and Hijmans (2017).
[f] PET = Potential Evapotranspiration (using the methods of Hargreaves et al., 1985), AI = Aridity Index, and WD = Water Deficit from Zomer et al. (2007, 2008).

the course of analysis was on average 0.15‰ (combined measure of accuracy and precision of the standard). Each sample was analyzed two or more times, and normalized to the VPDB isotopic scale using the multi-point A6-mix correction. The FAMEs were corrected for methyl group added during methylation and the results reported for each homologue in permil (‰). Hydrogen isotopic analyses of the plant wax homologues are reported in Appendix A.

2.3.3. Bulk soil carbon isotope analysis

Part of the soil samples were taken for total organic carbon (TOC) and bulk organic carbon isotopic ($\delta^{13}C_{SOM}$) analysis. The soils were decarbonated with HCl (10% v/v) in a 70 °C water bath for 2 h and then rinsed three times with deionized water. After decarbonation, the dried samples were analyzed by an Elemental Analyzer (Costech Analytical Technologies Inc. Valencia, CA, USA) connected to a Picarro G2131-i cavity ring-down spectroscopy (CRDS) for TOC and $\delta^{13}C$ OC. A USGS-40 standard (Glutamic Acid, −26.6‰ on the VPBD scale) was interspersed with replicates at different weights to set a calibration curve to calculate TOC, as well as an assessment of the precision in $\delta^{13}C_{SOM}$ measurements (determined to be better than 0.2‰).

2.3.4. Soil carbonate carbon isotope analysis

Allied with a study of novel triple oxygen isotopes and clumped isotopes (Beverly et al., 2021), pedogenic carbonates were collected and the traditional stable carbon isotopic data are reported here. Pedogenic carbonates were collected from soil Bk horizons at 0.2 m intervals where present (ranging from 0.4 to 1.6 m depth). Pedogenic carbonates were cracked open and drilled using a Dremel drill to target different morphologies in the larger nodules and coatings on clasts to understand the variability within nodules and between nodules. In some cases, the entire nodule was pulverized using a mortar and pestle for very small nodules (<2 mm). Stable isotope compositions of powdered carbonates ($\delta^{18}O$ and $\delta^{13}C$) were analyzed on a Nu Perspective with an online Nu Carb autosampler and digested in 100% H_3PO_4 at 90 °C. Corrections are based on a two-point calibration using the NBS-18 and NBS-19 calcite standards and normalized to the VPDB isotopic scale. The standard deviation for replicates of these standards analyzed with unknowns was <0.05‰ for $\delta^{18}O$ and <0.02‰ for $\delta^{13}C$.

3. RESULTS

3.1. Abundance of carbon archives within savanna soil

We first report plant wax and bulk organic concentrations across all soil samples. Σalk ranged from 0.09 to 5.05 μg/g (median = 0.79 μg/g) and Σacid was an order of magnitude greater, ranging from 0.40 to 70.92 μg/g (median = 9.93 μg/g). TOC ranged between 0.14 and 3.01% (median = 0.57%). Σalk, Σacid and TOC declined systematically with depth at almost all sites (Fig. 2a–c; data available at Feakins, 2020).

Normalizing Σalk and Σacid for TOC, we find Λalk ranges from 0.05 to 0.61 mg/g OC (median = 0.12 mg/g OC), and Λacid ranges from 0.15 to 11.01 mg/g OC (median = 1.74 mg/g OC). The decline in plant wax concentrations are proportional to that of TOC such that Λalk and Λacid, as well as the ratio of *n*-alkanes to *n*-alkanoic acids are relatively invariant with increasing depth.

Within compound classes, we found plant wax *n*-alkane homologues in soils ranging from C_{23} to C_{35} (carbon chain length) with the expected predominance of odd carbon number, long chain homologues ($CPI_{23\text{-}35}$ ranged from 3.9 to 8.5). Mid chain *n*-alkanes (often attributed to microbial production) are less abundant than long-chains, and do not systematically change within the soil depth profiles. In all samples, C_{29}, C_{31}, and C_{33} are the most abundant *n*-alkane homologues, with lesser concentrations of C_{35} *n*-alkanes ranging from 0.009 to 0.286 μg/g, on average 6% of Σalk and approximately a third that of C_{33} *n*-alkanes. $ACL_{23–35}$ ranged from 28.4 to 31.3. Concentrations of long chain *n*-alkanoic acids are dominated by C_{28}, C_{30}, and C_{32}. $ACL_{22–34}$ ranged from 27.6 to 31.0, while $CPI_{22–34}$ (the even chain predominance) ranged between 2.3 and 4.9.

All of the surveyed grassland sites contained soil carbonate, distributed at depths between 0.45 and 1.6 m below the surface (Fig. 2), where the organic components are diminished relative to the upper 0.1 m (Fig. 2a–c). Soil carbonates were absent from two out of three sites with substantial C_3 vegetation present (classified as closed treed shrubland, mixed open grassland to woodland and open grassed woodland; Reed et al., 2009).

3.2. Component carbon isotopic composition within soil profiles

3.2.1. Compound specific carbon isotopic composition of plant wax homologues

Describing the results for commonly reported chain lengths first, we find the $\delta^{13}C$ values of C_{29} *n*-alkanes ($\delta^{13}C_{29alk}$) vary from −29.5‰ to −20.0‰ (mean = −23.5 ‰, σ = 3.1‰, n = 25 samples). C_{30} *n*-alkanoic acids have $\delta^{13}C$ values from −27.6‰ to −18.1‰ (mean $\delta^{13}C_{30acid}$ = −21.1 ‰, σ = 2.6‰, n = 26). Thus, C_{29} *n*-alkanes are offset by ~−2‰ from the C_{30} *n*-alkanoic acids (mean offset $\delta^{13}C_{29alk} - \delta^{13}C_{30acid} = -2.3$‰, σ = 2.0 ‰, n = 25). In addition to these select homologues, we measured compound specific carbon isotopic values on the C_{25} to C_{35} odd chain length *n*-alkane homologues and the C_{22} to C_{34} *n*-alkanoic acid homologues (Fig. 3a), as well as their hydrogen isotopic compositions (see supplementary text in Appendix A), with all plant wax abundance and isotopic data available at Feakins (2020). Although the dataset is relatively small (n = 26 samples), correlations between homologues generally yield significant, positive relations; but there are notably weaker correlations for the (often low abundance) C_{25} and C_{35} *n*-alkane (Fig. 3b). Among all the long-chain C_{29}-C_{35} *n*-alkanes, and C_{28}-C_{34} *n*-alkanoic acids we find the C_{29} and C_{30} are generally the most depleted and variable of all the homologues ($\delta^{13}C_{29alk}$ −23.5 ± 3.1,

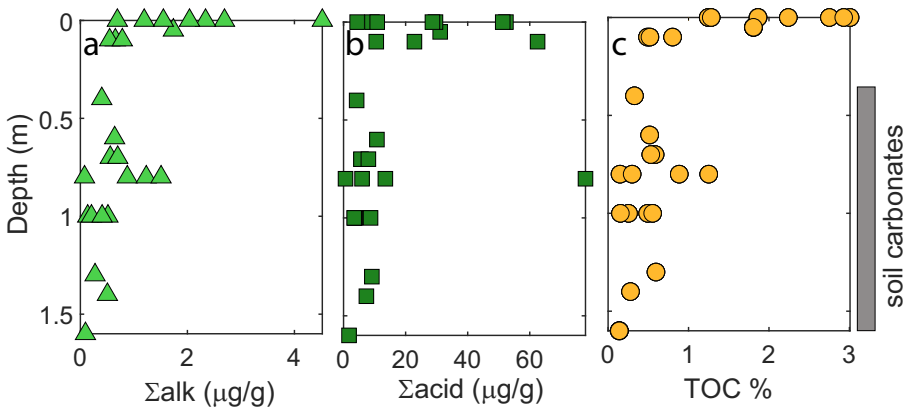

Fig. 2. Depth profiles compiling data from all sites across the Serengeti transect, showing the abundance of plant wax a) summed C_{23} to C_{35} *n*-alkanes (Σalk) and b) summed C_{22} to C_{34} *n*-alkanoic acids (Σacid); c) soil organic matter and depth distribution of sampled soil carbonate nodules.

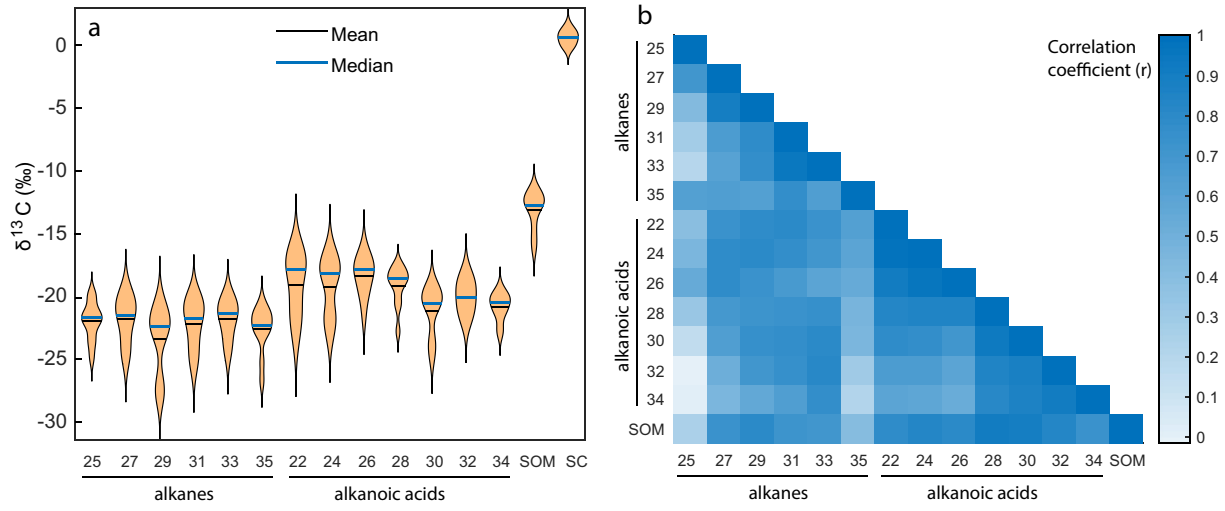

Fig. 3. (a) Violin plots showing the distribution of carbon isotopic compositions across all homologies and proxies for all sites and samples. (b) Correlogram or heatmap showing the Pearson correlation coefficients (r) for the relationships in $\delta^{13}C$ values between C_{25} to C_{35} *n*-alkanes, C_{22} to C_{34} *n*-alkanoic acid homologues and SOM for paired analyses.

$\delta^{13}C_{31alk}$ −22.2 ± 2.0, $\delta^{13}C_{33alk}$ −21.9 ± 1.8, $\delta^{13}C_{35alk}$ −22.6 ± 2.1, $\delta^{13}C_{28acid}$ −19.1 ± 2.1‰, $\delta^{13}C_{30acid}$ −21.1 ± 2.6‰, $\delta^{13}C_{32acid}$ −20.1 ± 1.7‰ and $\delta^{13}C_{32acid}$ −20.9 ± 1.9‰).

3.2.2. Offsets between plant wax homologues and SOM

The *n*-alkyl lipids are more ^{13}C-depleted than bulk soil organic matter (Fig. 3a). While all long chain (plant wax) *n*-alkanes and *n*-alkanoic acids are isotopically similar, they are more depleted compared to the mid-chain (microbial) C_{22}-C_{26} *n*-alkanoic acids (Fig. 3a). $\delta^{13}C_{SOM}$ values range from −18.4‰ to −11.2‰ (mean = −13.1‰, σ = 1.8‰, n = 26 samples). Comparing commonly reported plant wax homologues: C_{29} *n*-alkanes are depleted relative to SOM by ~−10‰ (mean $\Delta^{13}C_{29alk\text{-}SOM}$ = −10.3‰, σ = 1.9‰, n = 25) and the C_{30} *n*-alkanoic acid is offset from SOM by ~ −8‰ (mean $\Delta^{13}C_{30acid\text{-}SOM}$ = −8.0‰, σ = 1.3‰, n = 26). Comparison of longer chain homologues, the C_{31} and C_{33} *n*-alkane and C_{32} *n*-alkanoic acid with SOM yields smaller offsets of ~−9‰ (mean $^{13}C_{31alk}$ − $\delta^{13}C_{SOM}$ = −9.0‰, σ = 1.5‰, n = 25; mean $^{13}C_{33alk}$ − $\delta^{13}C_{SOM}$ = −8.7‰, σ = 1.4‰, n = 25) and ~−7‰ (mean $\delta^{13}C_{32acid}$ − $\delta^{13}C_{SOM}$ = −6.9‰, σ = 1.0‰, n = 26) respectively. Compared to offsets of −8‰ and −6‰, for C_{29} and C_{30} respectively, reported for soils under wet, tropical C_3 forests (Wu et al., 2019), we observe larger offsets under these relatively dry savanna settings.

We note the $\delta^{13}C_{29alk}$ and the $\delta^{13}C_{30acid}$ values are more negative than other homologues in three surface samples at Banagi, Makoma and Kemarishe, each sites with substantial C_3 vegetation present (two of which also do not contain soil carbonate nodules). We measure mean $\delta^{13}C_{29alk}$ = −29.1‰, σ = 0.4‰, versus $\delta^{13}C_{33alk}$ = −24.9‰, σ = 1.1 ‰ an offset ($\delta^{13}C_{29alk}$ − $\delta^{13}C_{33alk}$) of −4.2‰, whereas the mean offset of all other sites is −1.3‰. Similarly, the mean $\delta^{13}C_{30acid}$ −27.2‰, σ = 0.7 ‰ is more negative versus

$\delta^{13}C_{32acid}$ −23.5‰, $\sigma = 0.6$ ‰ at those three sites. Thus, the $\delta^{13}C_{29alk}$ and the $\delta^{13}C_{30acid}$ are not representative of their compound class when trees are present, whereas other homologues including the C_{31} and C_{33} *n*-alkanes and C_{33} *n*-alkanoic acids are robustly representative across all sampled vegetation types.

3.2.3. Depth profile comparison of organic components

Compiling organic data with depth across all sites, we find depth-dependency not only in the abundances (Fig. 2) but also in their carbon isotopic compositions (Fig. 4). We show data for a representative homologue of each compound class showing the C_{33} *n*-alkane (Fig. 4a) and the C_{32} *n*-alkanoic acid (Fig. 4b), as well as that of bulk organic carbon (Fig. 4c). We find $\delta^{13}C$ values are lower (and variable) at the surface and progressively higher at depth; this pattern is more pronounced in the *n*-alkanoic acids (Fig. 4b) compared to the *n*-alkanes (Fig. 4a). In SOM, surface soil ^{13}C-depletion is seen in only the three sites with significant C_3 tree cover today (Kemarishe, Makoma and Banagi; under closed treed shrubland, mixed open grassland to woodland and open grassed woodland respectively; Fig. 4c).

3.2.4. Soil carbonates

From the nine sites with soil carbonates, $\delta^{13}C_{SC}$ ranges from −2.7‰ to +1.8‰ (mean = 0.5 ‰, σ = 0.8‰, n = 70) (Fig. 4d). Most of that variability is nodule-to-nodule variability, as averaging the data by site, the variance is comparable (mean site standard deviation is σ = 0.8‰). In each soil pit, we sampled soil carbonate at 0.2 m depth intervals and found that when averaging the nodule data by depth within a site, the average standard deviation within discrete horizons is only σ = 0.3‰. We do not find any systematic depth-dependent pattern in $\delta^{13}C_{SC}$ (Fig. 4d). We compared the site mean $\delta^{13}C_{SOM}$ with the site mean $\delta^{13}C_{SC}$ (following Cerling and Quade, 1993) where:

$$\Delta^{13}C_{SC-SOM} = \delta^{13}C_{SC} - \delta^{13}C_{SOM} \quad (3)$$

$\Delta^{13}C_{SC\text{-}SOM}$ range from 11.9 to 15.5‰ (mean = 13.2‰, σ = 1.2‰, n = 9).

4. DISCUSSION

4.1. Comparison of organic proxies

4.1.1. Evaluating surface soil $\delta^{13}C$ archives under grasslands and wooded grasslands

The carbon isotope results from bulk organics in surface soils of the Serengeti transect (mean $\delta^{13}C_{SOM}$ −14.2‰, σ 2.2‰, n = 11) reflect dominant contributions from C_4 vegetation (Rieley et al., 1991; Rieley et al., 1993; Cerling et al., 2011). At the three sites with vegetation classifications indicating 20–50% tree cover (Banagi, Makoma and Kemarishe), ^{13}C-depleted surface SOM values, (~−17‰) indicate the presence of both C_3 and C_4 plants. For comparison, $\delta^{13}C_{SOM}$ values range from −12 to −28‰ in a global compilation across a range of woody cover from open C_4 grassland to closed canopy C_3 rainforest (Cerling et al., 2011) and bulk leaves average −26.4 ± 2.1‰ in C_3 plants (trees and most shrubs) and −11.4 ± 1.3‰ in C_4 plants (mostly grasses) collected from eastern and central Africa (Cerling, 2014).

Plant wax *n*-alkane and *n*-alkanoic acid carbon isotopic compositions across all 13 reported homologues, in surface samples at all 11 sites (mean = −21.8‰, 1 σ, 2.6‰, n = 137), suggest dominantly C_4 grass inputs, consistent with modern vegetation descriptions (Reed et al., 2009). The C_{29} *n*-alkane and C_{30} *n*-alkanoic acids, display low values of ~−28‰, indicative of mixed C_3 and C_4 plant inputs, i.e., a greater C_3 input to these homologues compared to other homologues. These lower values are found at three sites (Banagi, Kemarishe and Makoma); these are the only sites with C_3 trees present as observed in 2018, and classified in 2009 as closed treed shrubland, mixed open grassland to woodland, and open grassed woodland, respectively (Reed et al., 2009). For comparison to measured values on plants reported elsewhere in Africa: the average $\delta^{13}C$ values of plant wax *n*-alkanes measured in

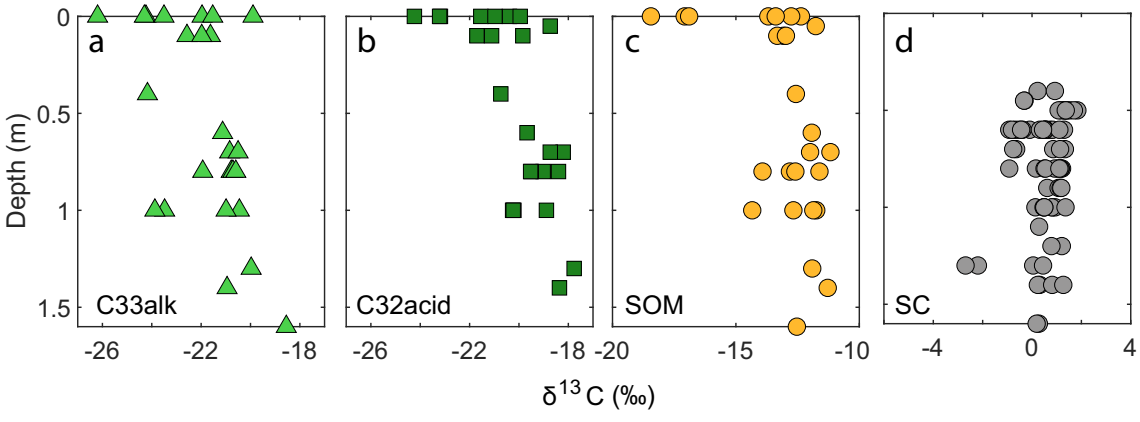

Fig. 4. Depth profiles compiling data from all sites across the Serengeti survey, showing the $\delta^{13}C$ values of plant wax a) C_{33} *n*-alkanes and b) C_{32} *n*-alkanoic acids; c) soil organic matter and d) soil carbonate nodules.

living C_4 grasses of the subfamilies Aristidoideae, Chloridoideae and Panicoidea sampled across Africa including Tanzania range from −25.2 to −19.1‰ (Rommerskirchen et al., 2006b) with plant wax *n*-alkanes of C_4 plants in savannas of Angola −22.0 ± 1.9‰ ($n = 33$), those of C_3 plants within those same ecosystems being −33.8 ± 2.3‰ ($n = 44$; Badewien et al., 2015) and plant wax *n*-alkanes of savanna woodland C_3 trees sampled throughout Africa are found to have values of −33.2 ± 2.4‰ ($n = 27$; Vogts et al., 2009).

While both plant wax homologues and SOM proxies yield similar evidence, compound specific approaches allow for the comparison across homologous series. While all homologues show a positive correlation in isotopic composition (Fig. 3), consistent with a common source, the lower abundance homologues (C_{25} and C_{35} *n*-alkanes) have lower correlations, suggesting some influence of differential sourcing, degradation or analytical artifacts. Differential sourcing may include more microbial inputs (representing degradation processes contributing to the shorter chain C_{25}) or more grass inputs to the long chain C_{35}, but analytical artifacts may be associated with their generally low concentrations, vulnerable to coelution and baseline influences – thus we avoid these homologues for interpretations.

Some homologue differences may be beneficial for interpretations. The observation of low $\delta^{13}C_{29alk}$ values in surface soils under 20–50% tree cover is consistent with a C_3 bias in this homologue. This fits with reports of the modal concentrations of C_{29} *n*-alkanes in tropical tree leaves (Garcin et al., 2014), whereas C_4 grasses have a modal concentration in the C_{33} *n*-alkanes (Rommerskirchen et al., 2006b). We find $\delta^{13}C_{29alk}$ values are particularly sensitive to woody cover, with offsets $\delta^{13}C_{29alk} - \delta^{13}C_{33alk}$ of up to −6‰ in samples with higher proportional concentrations of C_{29}. For example, in surface soils at Banagi, the measured $\delta^{13}C_{29alk}$ value of −29.5‰ offset by −5‰ from $\delta^{13}C_{33alk}$. If not correcting for differential homologue production in trees, use of $\delta^{13}C_{29alk}$ may lead to an underestimate of the proportional presence of grasses on the landscape. For some species, the C_{31} *n*-alkane also has high tree production (Garcin et al., 2014) though this is not strongly apparent here, with C_{31} being intermediate but closer to C_{33}. We wish to emphasize that $\delta^{13}C_{29alk}$ may be useful for diagnosing tropical tree expansion as pollen preservation is often poor in arid zones and tropical trees tend to be insect pollinated and thus produce low amounts of pollen (Bonnefille, 2010). When the goal is tropical tree detection, $\delta^{13}C_{29alk}$ is a responsive sensor, and the offset between C_{29} and C_{33} may be diagnostic of mixed C_3 and C_4 such as found in ecosystems with 20–50% tree cover sampled here. While *n*-alkanoic acids concentrations patterns have not yet been adequately described in C_4 grasses, there are signs that tropical trees often show a modal C_{30} *n*-alkanoic acid abundance (Feakins et al., 2016a). As the C_{30} *n*-alkanoic acid pattern mimics that of C_{29} *n*-alkane, we suggest C_{30} may also be sensitive to tree inputs.

Elsewhere the isotopic range of C_{27} to C_{33} *n*-alkanes (leaf wax isotopic spread; LEWIS) has been proposed as a measure of plant diversity (Magill et al., 2019). In this study we find the C_{29} *n*-alkane is depleted relative to other homologues at sites with trees, as would be simply explained by greater tree production of that homologue (Garcin et al., 2014). While LEWIS yields a similar magnitude, LEWIS is non-directional i.e. the same value could be achieved by tree depletion or by petrogenic enrichment of C_{29} relative to other homologues. Thus, we present directional offsets monitoring for tree inputs by the isotopic offset between C_{29} and C_{33} *n*-alkanes, as would be predicted by their differential production (Garcin et al., 2014).

Homologues that are not dominated by tree production (e.g., the C_{33} *n*-alkane; Garcin et al., 2014), may best reflect proportional changes between grasses and trees. For example, $\delta^{13}C_{33alk}$ has been found to be sensitive to C_3/C_4 vegetation changes as reported from a downcore study of a marine sediment core at the mouth of the Zambezi River in SW Africa (Wang et al., 2013). Elsewhere, $\delta^{13}C_{35alk}$ has been suggested to be a stronger sensor for the Neogene C_4 expansion than $\delta^{13}C_{29alk}$ (Uno et al., 2016b; Polissar et al., 2019; Polissar et al., 2021). However, lycopane, a marine derived biomarker with high $\delta^{13}C$ values, can coelute with C_{35}, and thus, an increase of both abundance and isotopic composition could be due to lycopane production (Sinninghe Damsté et al., 2003; Schefuss and Dupont, 2020). Furthermore, the typically low abundances of C_{35} relative to C_{33} *n*-alkanes in C_4 grasses of the subfamilies Aristidoideae, Chloridoideae and Panicoidea sampled across Africa (Rommerskirchen et al., 2006b) makes the attribution of the C_{35} peak to grasses even more tenuous in contrast to North American C_4 grasses (Bush and McInerney, 2013). We also note that the C_{35} is lower abundance relative to C_{33} in these Serengeti C_4 grassland soils than in tropical rainforest trees surveyed in Peru (Feakins et al., 2016b), such that regional ecological differences matter more than life form. The low abundance of the C_{35} homologue (C_{35} is a third of C_{33} abundance in this study) presents a challenge for robust determinations of $\delta^{13}C_{35alk}$ (precision and accuracy of isotopic determinations may be lower), such that their isotopic values are usually not reported. We suggest any other popular long chain *n*-alkane and *n*-alkanoic acid homologues are suitable (e.g., $\delta^{13}C_{31alk}$) and in particular recommend $\delta^{13}C_{33alk}$, as a robust proxy across woody and grassy ecosystems, in agreement with Wang et al., (2013); C_{29} already having been shown to be tree-biased by Garcin et al., (2014) and reinforced here.

4.1.2. Depth profiles of soil organic matter and their carbon isotopic signatures

The depth profiles of organic concentrations of plant waxes and SOM (Fig. 2) are as expected and are analogous to the depth profiles of SOM reported from US grassland soils (Retallack, 1991). The concentrations are low (<1% TOC) below the comparatively organic-rich surface horizons (A horizon, <3% TOC), consistent with dominantly surface inputs of organic matter (Fig. 2). Inputs are either directly from plant matter leaf litter, or via the dung of grazing herbivores, with mixing into the surface soil by dung beetles and to deeper depths principally by termites in the Serengeti (de Wit, 1978). The low concentrations of organics at depths down to 1.6 m sampled here, presumably

represent residuals from earlier inputs (Retallack, 1991), overprinted with contemporary additions from downward mixing (by insects) or minor below-ground additions from roots or microbial metabolism. Although we have no constraints on the age of organics here, studies elsewhere have shown that on average deeper organics are older (mostly multi-centennial to multi-millennial inputs) compared to the upper organic-rich layer that comprises more recent inputs (Schmidt et al., 2011). Analysis of the age distribution of organics in soil profiles globally has suggested that about 80% of SOC is found in the upper 0.3 m (topsoil) with about 45% of that carbon being <50 years old, compared to just 13% of the SOC in 0.3–1 m (Balesdent et al., 2018). The older organic components tend to be more degraded (Wynn et al., 2005), and elsewhere, this results in a ^{13}C-enrichment in the deeper SOC by up to 6‰ relative to original biomass in the products of microbial decomposition (Wynn, 2007).

Roots have been shown to influence below-ground carbon in the vicinity of root structures, although roots are generally calculated to be negligible contributors to soil OM in a series of loess studies in Europe including studies of bulk and plant wax compounds (Gocke et al., 2013, 2014; Häggi et al., 2014). In this setting within 1.6 m soil pits, roots typically were densely present in the upper 0.4 m above the calcite similar to reports of de Wit (1978) and rarely were roots noted at greater depths, associated with higher salinities and alkalinities at depth (de Wit, 1978). As we see no features in the organic profiles at the base of rooting, we infer that roots are unlikely to be a major influence on the organic archives.

Evaluating the carbon isotopic composition of organic matter across the depth profiles, we find surface soils are generally ^{13}C-depleted relative to mid-depth samples, as shown for the $\delta^{13}C_{29alk}$, $\delta^{13}C_{30acid}$ and $\delta^{13}C_{SOM}$ (Fig. 5). At the C_4 grassland sites ($n = 8$), median offsets of surface soils are offset from mid-depth samples by −1.4‰, −2.3‰ and −0.8‰ in $\delta^{13}C_{29alk}$, $\delta^{13}C_{30acid}$ and $\delta^{13}C_{SOM}$ respectively (selecting the median as the mean is skewed by the change in a few sites). Assuming the surface organic-rich layer reflects mostly recent inputs, and the deeper organic-lean layers represents older inputs, as seems likely in these undisturbed soil profiles, then we suggest the surface depletion results at least in part from the Suess effect, i.e. the ^{13}C-depletion of the atmospheric CO_2 as a result of fossil fuel burning. The magnitude of this atmospheric effect is ~2‰ considering the date of soil collection (2018) relative to pre-Industrial (Friedli et al., 1986; Keeling et al., 2001) of which ~1‰ occurred in the last few decades. Higher pCO_2 can also drive fractionation changes adding modestly to this effect (Schubert and Jahren, 2012), although plant stomata may adjust to counteract this effect. However, due to the long duration of soil surfaces and the mixing processes within soils, surface soil OM is not all modern (multi-decadal) and the deeper soil is not all pre-Industrial and this mixed age composition would dampen the soil profile record of changing inputs related to the Suess effect to likely <1‰. Thus, we suspect the ^{13}C-depletion of surface soils under grasslands likely represents the combined effects of the change in atmospheric composition and a recent undetected change in vegetation cover, such as additions of C_3 forbs within the grasses, as well as a tendency for ^{13}C-enrichment at depth with degradation of those older components (Wynn et al., 2005; Wynn, 2007).

4.1.3. Soil profiles identify C_3 encroachment into C_4 grasslands

The largest surface soil ^{13}C-depletions occur at sites with substantial C_3 vegetation present today: Banagi, Kemarishe and Makoma, classified as closed treed shrubland, mixed open grassland to woodland and open grassed woodland respectively by Reed et al. (2009), based on classification surveys in 1998–2002. Each of those three sites has surface soil offsets from mid-depth values by −2.8‰, −5.5‰ and −4.1‰ in $\delta^{13}C_{29alk}$ and $\delta^{13}C_{30acid}$ values and $\delta^{13}C_{SOM}$ respectively (Fig. 5). These surface soil ^{13}C-depletions exceed the magnitude seen in other soil profiles in the region (Fig. 5). Although sites with 20–50% tree cover may support greater soil biological activity and thus a larger degradation effect, we see no difference in the abundance of organics in the soil profiles. Thus, we suggest the carbon isotope profiles are consistent with an increase in woody cover in recent decades at Banagi, Kemarishe and Makoma, similar to findings of woody encroachment into C_4 grasslands from soil organic matter carbon isotopic profiles in Australia (Krull et al., 2005). The encroachment of woody plants on savannas is a widely-reported phenomenon, linked primarily to the increasing pCO_2 in the global atmosphere, despite local differences in land management practices (Stevens et al., 2017). While eastern African grasslands have been classified as climatically-determined low tree cover (Staver et al., 2011), they may be close to bistability, i.e. allowing for either grasslands or woodlands (Higgins and Scheiter, 2012) and supporting evidence for instability comes from Tsavo National Park, Kenya, where pollen show changing tree/grass proportions over the last 1,300 years (Gillson, 2004). Reduced disturbance, whether a reduction of browsing or fire suppression, can contribute to tree recruitment in savannas (Staver et al., 2011), in addition to the C_3 tree promotion by global atmospheric pCO_2 rise. The extent of vegetation change in the Serengeti is not well known as the last time the vegetation was mapped was 20 years ago 1998–2002 (Reed et al., 2009). Our carbon isotopic evidence for woody (or other C_3) encroachment is therefore an interpretation that can be tested with vegetation surveys.

4.1.4. Calibration of the carbon isotopic composition of plant wax to that of SOM

Although the $\delta^{13}C$ distributions of C_3 and C_4 plants do not overlap, their spread is broad with >15‰ range in C_3 plants and >5‰ in C_4 plants (Cerling, 2014), precluding efforts at unique C_4% solutions from the $\delta^{13}C$ values of sedimentary mixtures. While there is no single 'endmember' for C_3 plants, this manuscript does constrain a characteristic C_4 African grassland endmember in a range of materials.

$\delta^{13}C_{SOM}$ has recently been quantitatively linked to fractional woody cover (f_{wc}), using a polynomial relationship observed in a database of soils spanning several continents

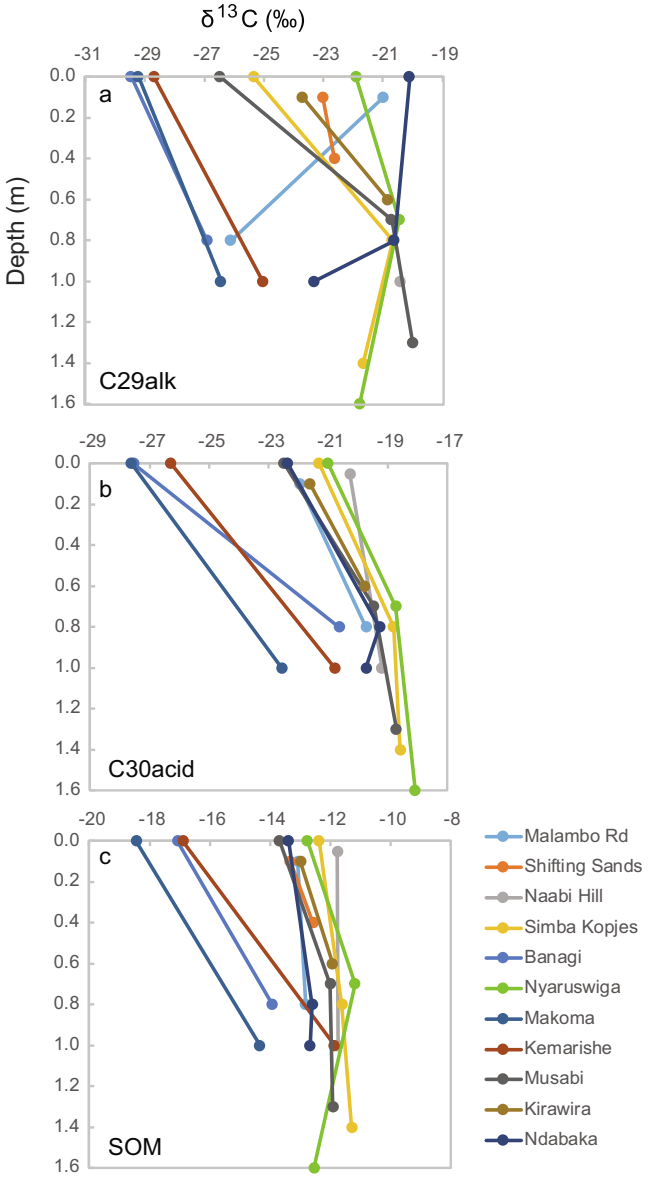

Fig. 5. Soil depth profiles showing a) $\delta^{13}C_{29alk}$, b) $\delta^{13}C_{30acid}$, and c) $\delta^{13}C_{SOM}$. There is a general tendency for surface soils to be ^{13}C-depleted, especially at the three sites with C_3 influence today (Makoma, Banagi and Kemarishe).

(Cerling et al., 2011). Here we seek to relate plant wax $\delta^{13}C$ values to that of $\delta^{13}C_{SOM}$ in order to leverage the larger global $\delta^{13}C_{SOM}$ dataset compiled by Cerling et al. (2011) when evaluating plant wax carbon isotopic data in terms of woody cover. In order to expand the calibration of plant wax carbon isotopic composition in soils across a broader range of vegetation types, we surveyed the published literature for available data on soil organic matter, *n*-alkanes and *n*-alkanoic acids, where all three measurements were present in the same soil samples. The C_{29} *n*-alkanes and C_{30} *n*-alkanoic acids were selected as they are most commonly reported. Combination of data from the present study and previously published data from tropical forest soils in the Amazon, woodland and woody grassland of Australia, and agricultural fields of France and Germany (Cayet and Lichtfouse, 2001; Wiesenberg et al. 2004; Krull et al., 2006; Wu et al., 2019), provides a dataset comprising 47 soil samples (Fig. 6).

We find that plant wax $\delta^{13}C$ values have a significant, positive correlation with $\delta^{13}C_{SOM}$ for both the $\delta^{13}C_{29alk}$ ($y = 0.86x - 12.18$, $r^2 = 0.91$, $n = 47$, $p < 0.0001$) (Fig. 6a) and $\delta^{13}C_{30acid}$ ($y = 1.02x - 5.89$, $r^2 = 0.97$, $n = 43$, $p < 0.0001$) (Fig. 6b). This comparison of the carbon isotopic composition of SOM and plant wax *n*-alkanes and *n*-alkanoic acids in soils, spans the full carbon isotopic range from ^{13}C-depleted rainforests across a range of C_3 ecosystems from the prior literature, with this Serengeti study defining the C_4 grassland extreme. Global coverage is sparse at this time, and would ideally be expanded with future multi-proxy measurements on soils from a

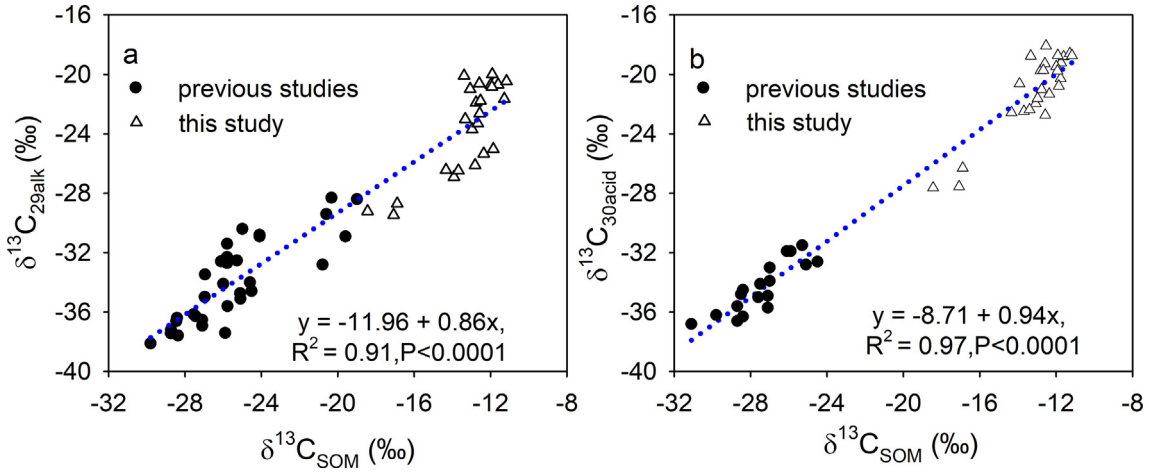

Fig. 6. Comparing the relationships between $\delta^{13}C_{SOM}$ and a) $\delta^{13}C$ of C_{29} *n*-alkane and b) C_{30} *n*-alkanoic acid showing data from the Serengeti transect (this study, triangles) and previous studies (circles). The previously published data in (a) were compiled from available published data with paired carbon isotopic analyses of plant wax C_{29} *n*-alkane and SOM reported from soils under tropical rainforests in the Amazon (Wu et al., 2019), woodlands and woody grasslands of Australia (Krull et al., 2006), and agricultural fields in France and Germany (Cayet and Lichtfouse, 2001; Wiesenberg et al. 2004), mostly under C_3 plants, while the Serengeti grasslands constrains the soils under mostly C_4 plants with some C_3 influenced sites to which C_{29alk} is shown to be 'oversensitive' (this study). For the C_{30} *n*-alkanoic acid and SOM comparison in (b) these data were only available from tropical rainforests (Wu et al., 2019, circles) and the Serengeti grasslands (this study). The positive, orthogonal linear regressions ($0.9 < r < 1$, $p < 0.001$) indicate the strong, significant relationships between $\delta^{13}C_{SOM}$ and $\delta^{13}C$ of C_{29} *n*-alkanes and C_{30} *n*-alkanoic acids.

range of ecosystems around the world, including the grasslands of other continents, as species, climates and community structures may affect carbon isotopic fractionations.

Using these relationships between plant wax homologues and SOM (Fig. 6) and the global calibration of SOM to f_{wc} (Cerling et al., 2011):

$$\delta^{13}C_{SOM} = -9.02\arcsin(\sqrt{f_{wc}} - 14.49) \quad (4)$$

we can then relate plant wax $\delta^{13}C$ archives to predict woody cover. We calculate the proportion of woody cover in these soil samples based on the measured carbon isotopic composition of the various archives (SOM, plant wax *n*-alkane and *n*-alkane homologues) to test for equivalency. Using measured $\delta^{13}C_{SOM}$ we find f_{wc} ranges from 0.00 to 0.18 (mean = 0.06, $\sigma = 0.04$, $n = 26$) consistent with expectations for C_4 grasslands and wooded grasslands. The match suggests that $\delta^{13}C_{SOM}$ is a faithful recorder of modern vegetation and that vegetation has been stable during the period of soil formation represented in these depth profiles.

As we found that the isotopic range of plant wax homologues and SOM differed, we found a uniform difference term or epsilon was not sufficient for comparison between archives. We therefore used a regression to handle the problem of "scale compression" in the SOM relative to the greater variance in the plant wax homologues. Using the regression between plant wax ($\delta^{13}C_{29alk}$ or $\delta^{13}C_{30acid}$) with $\delta^{13}C_{SOM}$ (Fig. 5) we can convert the plant wax values to the SOM scale:

$$\delta^{13}C_{29alk-SOM} = (\delta^{13}C_{29alk} + 11.96)/0.86 \quad (5)$$

$$\delta^{13}C_{30acid-SOM} = (\delta^{13}C_{30acid} + 8.71)/0.94 \quad (6)$$

and then employ these converted values in Eq. (4) to calculate f_{wc}. Based on measured $\delta^{13}C_{29alk}$ f_{wc} ranges from 0.00 to 0.64 (mean = 0.33, $\sigma = 0.24$, $n = 25$), with the highest f_{wc} (0.64) falling in the range of woodlands, which is an overestimate of tree cover by at least 14% compared to vegetation classifications. Using $\delta^{13}C_{30acid}$ we find f_{wc} ranges from 0.01 to 0.35 (mean = 0.16, $\sigma = 0.10$, $n = 26$), indicating a maximum f_{wc} that would be within the wooded grassland range and therefore attributes to the correct category, but with double the woody cover of that indicated by $\delta^{13}C_{SOM}$.

While global regression calibrations for $\delta^{13}C_{33alk}$ and $\delta^{13}C_{32acid}$ to SOM are lacking, mean offsets ($\Delta^{13}C_{32acid\text{-}SOM}$ and $\Delta^{13}C_{32acid\text{-}SOM}$) from all 26 samples are available to adjust individual measured $\delta^{13}C_{33alk}$ and $\delta^{13}C_{32acid}$ to the equivalent SOM scale:

$$\delta^{13}C_{33alk-adj} = (\delta^{13}C_{33alk} + \Delta^{13}C_{32acid-SOM}) \quad (7)$$

$$\delta^{13}C_{32acid-adj} = (\delta^{13}C_{32acid} + \Delta^{13}C_{32acid-SOM}) \quad (8)$$

Using this approach, $\delta^{13}C_{33alk}$ yields f_{wc} ranges from 0.00 to 0.18 (mean = 0.06, $\sigma = 0.04$, $n = 25$) and $\delta^{13}C_{32acid}$ ranges from 0.00 to 0.18 (mean = 0.06, $\sigma = 0.04$, $n = 26$). Thus, we find equivalent predictions from $\delta^{13}C_{SOM}$, $\delta^{13}C_{33alk}$ and $\delta^{13}C_{32acid}$ for all sites, whereas the $\delta^{13}C_{29alk}$, and to a lesser extent the $\delta^{13}C_{30acid}$, overestimate f_{wc}.

4.2. Comparison of organic and carbonate proxies

4.2.1. Comparison of organic and soil carbonate evidence under (wooded) grasslands

Soil carbonates can only be found in restricted climate zones: they may precipitate in soils under arid to subhumid climatic conditions when sufficient calcium is present (Cerling, 1984). Nevertheless, soil carbonates have contributed abundant data to reconstructions of landscapes

across hominin sites (Levin et al., 2004, 2011; Cerling et al., 2011) and to reconstructions of temporal change in ecosystems over time (Quade et al., 1989; Cerling, 1992). However, carbonates do not precipitate in soils in more humid climates and thus are absent from many paleosols – in those cases the organic approaches (whether bulk or compound specific) can fill the data gap.

In the Serengeti soil profiles pedogenic carbonates were found at 0.4–1.6 m depth. At most sites, pedogenic carbonates capture a signal of the dominantly C_4 grassland vegetation above. $\delta^{13}C_{SC}$ values of −0.04‰ ($\sigma = 0.76$, $n = 11$) at Banagi, and −0.70‰ ($\sigma = 0.08$, $n = 2$) at Nyaruswiga suggesting some C_3 influence at those two sites, as expected from their vegetation classifications (mixed open grassland to woodland and open treed grassland to closed grassland respectively). Pedogenic carbonates are not found at Makoma and Kemarishe, two of the sites with C_3 woody cover, thus the soil carbonates do not capture a record of the C_3 vegetation at those sites (illustrating the need for organic proxies in such settings).

More broadly, it is rare to find soil carbonates in tropical C_3 forest or woodland ecosystems today (Fig. 4; Cerling et al, 2011). A broader range of $\delta^{13}C_{sc}$ can be found in the geological record. For example, $\delta^{13}C_{sc}$ ranging from −13 to +3‰ were found in paleosols of the Siwalik formation in Pakistan spanning the last 17 Ma, indicating a late Miocene transition from C_3 to C_4 vegetation (Quade et al., 1989). After the expansion of C_4 ecosystems in the tropics, C_3 grasslands are restricted to higher elevations and higher latitudes, where soil carbonate forming conditions and climates are rare.

In contrast to the depth distribution of soil carbonates (0.4–1.6 m depth here), plant wax biomarkers and bulk organic matter are found with declining concentration with depth reflecting inputs at the surface (Fig. 2a,b) and lower concentrations at depth associated with downward mobilization and degradation. We found no relationship between the $\delta^{13}C_{SC}$ values of nodules and clast coatings and organic proxies from the closest horizon. In part the lack of correlation derives from the difference in variance. In contrast to the 6.5‰ range in $\delta^{13}C_{29alk}$, 4.2‰ range in $\delta^{13}C_{30acid}$, and 2.7‰ range $\delta^{13}C_{SOM}$, $\delta^{13}C_{SC}$ values exhibit the smallest range in values, <2.5‰. We note that the offset of $\delta^{13}C_{SC}$ from $\delta^{13}C_{SOM}$, is smaller (range 11.9–15.5‰, mean = 13.2‰, $\sigma = 1.2$‰, $n = 9$) than stated expectations of +15.5‰ (14–17‰), if soil carbonates formed in equilibrium with respired CO_2 from decomposing organic matter (Cerling and Quade, 1993). The differences may be explained by the timescale of integration, with hard nodules and clast coatings thought to incorporate 500–1000 years (Targulian and Krasilnikov, 2007), whereas organics reflect more recent inputs as there is microbial loss of the older components over time (Schmidt et al., 2011). The greater time averaging of soil carbonates likely explains the smaller range of observed variability compared to biomarkers.

We did not find systematic enrichment or depletion in soil carbonate nodules between depth horizons likely because no soil carbonate was found above 0.4 m. Below the soil-air interface at 0.4–0.5 m, soil carbonate is forming in equilibrium with soil CO_2 and previous studies have shown little variability below 0.5 m depth (Quade et al., 1989; Cerling and Quade, 1993; Breecker et al., 2009). The variability between nodules collected from the same depth is similar to previously reported variability and reflects local soil variability. Overall the values obtained are as expected under C_4 grasslands, and all pedogenic

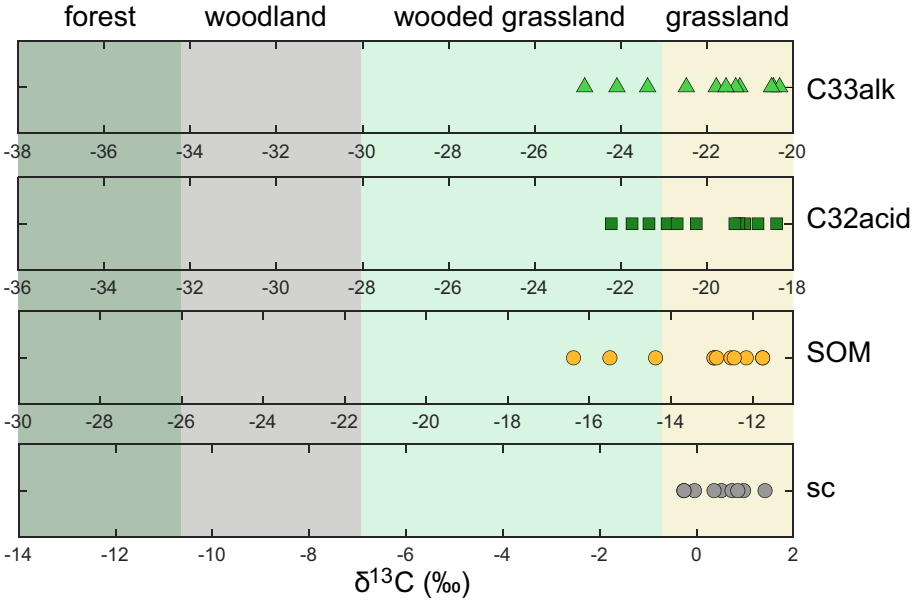

Fig. 7. Comparison of site mean values for four carbon isotopic archives against the expected range of values in the C_3-C_4 range (full x-axis) and the approximate ranges for vegetation types: forest, woodland, wooded grassland and grassland (color shading) – for soil carbonates and SOM the boundaries derive from Cerling et al. (2011), for plant waxes the bounds are set to accommodate this data as well as plants and lake sediments samples across a range of ecosystems in West Africa (Vogts et al., 2009; Garcin et al., 2014, Badewien et al., 2015) although rainforest trees can extend to more ^{13}C-depleted than shown.

carbonates would fall into the category of grassland by applying the $\delta^{13}C_{SC}$ values to the Fractional Woody Cover equation developed by Cerling et al. (2011), with the exception of two nodules from Musabi, which fall in the range expected for wooded grasslands (Fig. 7D).

In contrast we do find depth patterns in the organics: deep soil organic matter has a C_4 signature and plant wax biomarkers have a ^{13}C-depletion toward the surface. As discussed previously (Section 4.1.2), the pattern has been attributed to ^{13}C-depletion and pCO_2 increase of the atmosphere as well as inputs from C_3 trees at some sites. As C_4-like $\delta^{13}C_{SC}$ values are found in these soils, the longer-term integration of soil carbonate nodules (500–1000 years) also supports interpretation of the C_3 tree encroachment being recent.

4.2.2. Implications for paleoecological reconstructions

This study of multiple soil materials recording the carbon isotopic signature of C_4 grasslands in eastern Africa helps to show how four proxies archive the evidence for the same vegetation inputs. This survey is directly relevant to how the grassland ecosystem is recorded by each of four carbon isotopic proxies with regional applications, including soil carbonate and bulk organics (Cerling et al., 2011), plant wax *n*-alkanes (Magill et al., 2013) and *n*-alkanoic acids (Lupien et al., 2018; Saylor et al., 2019) in eastern African sites. The comparison reveals how the transient changes such as the Suess effect or woody encroachment appear in the organic soil profiles today, but are not detected in the soil carbonates that are known to have a longer time of formation.

These soils likely would contribute plant waxes to proximal sedimentary archives including Lake Victoria, whether via some surface stream incision or by dust deflation, from dry season or post-fire exposed soils. Indeed, we find concordance between the mean $\delta^{13}C$ value for the C_{29} *n*-alkane in these Serengeti soils (−23.5‰) to the majority of the Holocene lake record (~−24‰), which at times dips to −27‰ consistent with mixed grass and tree inputs (Berke et al., 2012).

5. CONCLUSIONS

This Serengeti soil survey evaluates the carbon isotopic composition of plant wax *n*-alkanes and *n*-alkanoic acids, together with bulk soil organic matter and soil carbonate nodules within the same soil profiles. These landscapes are dominantly C_4 grasslands with some C_3 trees, and we find all four proxies record the dominance of the grassland ecosystem, despite likely differences between their timescales of integration, suggesting a generally stable ecosystem during the timescale of soil formation. Soil carbonates provide consistent evidence for C_4 across the depth profiles and sites, but are absent at sites with trees. Bulk organics and plant wax *n*-alkane and *n*-alkanoic acid homologues are equivalent recorders at all grassland sites, with a ^{13}C depletion in surface soils linked to both the Suess effect on recent inputs and degradation at depth. At sites with trees, the C_{29} *n*-alkane (and to a lesser extent the C_{30} *n*-alkanoic acid) was found to overestimate tree cover, consistent with prior reports of molecular abundance distributions in trees (Garcin et al., 2014). The C_{29} *n*-alkanes show a greater surface soil ^{13}C-depletion than other homologues and this contrast may be useful in soil profiles as a sensitive detector of tree encroachment (Krull et al., 2005). All other homologues are equivalent recorders in these C_4 grasslands. Based on molecular abundance and carbon isotopic consistency, we recommend C_{31} and C_{33} *n*-alkanes and C_{32} *n*-alkanoic acid for similar tropical savanna paleovegetation reconstructions. We advise against use of C_{35} *n*-alkanes (cf. Uno et al., 2016b; Polissar et al., 2019; Polissar et al., 2021), which are low abundance in these pure C_4 grasslands, and that have been previously been shown in marine settings to be prone to coelution from lycopane (Sinninghe Damsté et al., 2003), whose marine signal is indistinguishable from C_4. All other homologues of plant wax *n*-alkanes and *n*-alkanoic acids, bulk organics and soil carbonates are equivalent recorders in soils *in situ* under C_4 grassland. While soil carbonate, organic and plant wax proxies are interchangeable recorders in these modern soils *in situ* under C_4 grassland, differences that may arise in other settings may warrant multi-proxy approaches (Sarangi et al., 2021) and differential timescales of the proxy recorders warrants further investigation in soils and paleosols. Plant wax proxies in addition offer the possibility to extend reconstructions to soils and paleosols without carbonates and –after erosion by water or wind– to fluvial, lake and marine depositional archives. We hope that this multi-material investigation helps to encourage more substrate comparisons that often necessitate inter-lab collaborations, and among the plant wax studies to see more multi-homologue and compound class reporting across ecosystems and archives.

Declaration of Competing Interest

The authors declare that they have no known competing financial interests or personal relationships that could have appeared to influence the work reported in this paper.

ACKNOWLEDGEMENTS

This project was funded in part by the National Science Foundation EAR Postdoctoral Fellowship (EAR-PF-1725621) and University of Michigan for the field work and the analytical work that focused on soil carbonates. The China Scholarship Council funded the participation of Daolai Zhang and the University of Southern California supported the organic geochemistry laboratory research at USC. Thanks to Joseph Masoy and Honest Ndoro for field assistance. Samples were collected under permits issued to Beverly by the Tanzanian government under COSTECH Permit #2018-39-NA-2018-17, TANAPA Research Permit #: TNP/HQ/C.10/13, and TAWIRI Permit #: TWRI/RS-342/2016/116. This manuscript was improved through the helpful comments of three anonymous reviewers.

RESEARCH DATA

Research Data for the organic and plant wax carbon and hydrogen isotopic data associated with this article can be accessed at https://doi.org/10.1594/PANGAEA.921002. Soil carbonate carbon and oxygen isotopic data associated with Beverly et al. (2021) can be accessed at http://doi.org/10.5281/zenodo.4919027.

APPENDIX A. SUPPLEMENTARY MATERIAL

Supplementary information to this article can be found online at https://doi.org/10.1016/j.gca.2021.07.005. These supplementary materials include text, a table and a figure relating to paired hydrogen isotopic analyses of plant wax biomarkers.

REFERENCES

Badewien T., Vogts A. and Rullkötter J. (2015) *n*-Alkane distribution and carbon stable isotope composition in leaf waxes of C_3 and C_4 plants from Angola. *Org. Geochem.* **89-90**, 71–79.

Balesdent J., Basile-Doelsch I., Chadoeuf J., Cornu S., Derrien D., Fekiacova Z. and Hatté C. (2018) Atmosphere-soil carbon transfer as a function of soil depth. *Nature* **559**(7715), 599–602.

Berke M. A., Johnson T. C., Werne J. P., Grice K., Schouten S. and Damste J. S. S. (2012) Molecular records of climate variability and vegetation response since the Late Pleistocene in the Lake Victoria basin, East Africa. *Quat. Sci. Rev.* **55**, 59–74.

Beverly E., Levin N. E., Passey B. H., Aron P. G., Yarian D. A., Page M. and Pelletier E. M. (2021) Triple oxygen and clumped isotopes in modern soil carbonate along an aridity gradient in the Serengeti, Tanzania. *Earth Planet. Sci. Lett.* **567**, 116952.

Bonnefille R. (2010) Cenozoic vegetation, climate changes and hominid evolution in tropical Africa. *Global Planet. Change* **72**, 390–411.

Breecker D. O., Sharp Z. D. and McFadden L. D. (2009) Seasonal bias in the formation and stable isotopic composition of pedogenic carbonate in modern soils from central New Mexico, USA. *Bull. Geol. Soc.* **121**(3-4), 630–640.

Bush R. T. and McInerney F. A. (2013) Leaf wax n-alkane distributions in and across modern plants: Implications for paleoecology and chemotaxonomy. *Geochim. Cosmochim. Acta*, 161–179.

Cayet C. and Lichtfouse E. (2001) δ13C of plant-derived n-alkanes in soil particle-size fractions. *Org. Geochem.* **32**(2), 253–258.

Cerling T. E. (1984) The stable isotopic composition of modern soil carbonate and its relationship to climate. *Earth. Planet. Sci. Lett.* **71**, 229–240.

Cerling T. E. (1992) Development of grasslands and Savannas in East-Africa during the neogene. *Palaeogeog. Palaeoclim. Palaeoecol.* **97**(3), 241–247.

Cerling T. (2014) Stable isotope evidence for hominin environments in Africa. In *Treatise on geochemistry* (eds. K. Turekian and H. Holland), 2nd edition, pp. 157–167.

Cerling T. E. and Quade J. (1993) Stable carbon and oxygen isotopes in soil carbonates. In *Climate Change in Continental Isotopic Records* (eds. P. K. Swart, K. C. Lohmann, J. Mckenzie and S. Savin), pp. 217–231.

Cerling T. E., Wynn J. G., Andanje S. A., Bird M. I., Korir D. K., Levin N. E., Mace W., Macharia A. N., Quade J. and Remien C. H. (2011) Woody cover and hominin environments in the past 6 million years. *Nature* **476**, 51–56.

De Wit H. A. (1978) *Soils and grasslands of the Serengeti Plain* PhD Thesis. Communications Agricultural University, Wageningen, NL, p. 300.

Diefendorf A. F. and Freimuth E. J. (2017) Extracting the most from terrestrial plant-derived *n*-alkyl lipids and their carbon isotopes from the sedimentary record: a review. *Org. Geochem.* **103**, 1–21.

Ehleringer J., Sage R., Flanagan L. and Pearcy R. (1991) Climate change and the evolution of C_4 photosynthesis. *Trends in Ecol. Evol.* **6**, 95–99.

[dataset] Feakins, Sarah J. (2020) Plant wax n-alkane and n-alkanoic acid abundances, carbon and hydrogen isotopic compositions in eleven soil profiles along a Serengeti transect. PANGAEA, https://doi.org/10.1594/PANGAEA.921002.

Feakins S. J., Bentley L. P., Salinas N., Shenkin A., Blonder B., Goldsmith G. R., Ponton C., Arvin L. J., Wu M. S., Peters T., West A. J., Martin R. E., Enquist B. J., Asner G. P. and Malhi Y. (2016a) Plant leaf wax biomarkers capture gradients in hydrogen isotopes of precipitation from the Andes and Amazon. *Geochim. Cosmochim. Acta* **182**, 155–172.

Feakins S. J., Levin N. E., Liddy H. M., Sieracki A., Eglinton T. I. and Bonnefille R. (2013) Northeast African vegetation change over 12 m.y. *Geology* **41**(3), 295–298.

Feakins S. J., Liddy H. M., Tauxe L., Galy V., Feng X., Tierney J. E., Miao Y. and Warny S. (2020) Miocene C_4 grassland expansion as recorded by the Indus Fan. *Paleoceanogr. Paleoclimatol.* **e2020PA003856**.

Feakins S. J., Peters T., Wu M. S., Shenkin A., Salinas N., Girardin C. A. J., Bentley L. P., Blonder B., Enquist B. J., Martin R. E., Asner G. P. and Malhi Y. (2016b) Production of leaf wax *n*-alkanes across a tropical forest elevation transect. *Org. Geochem.* **100**, 89–100.

Feakins S. J., Wu M. S., Ponton C., Galy V. and West A. J. (2018) Dual isotope evidence for sedimentary integration of plant wax biomarkers across an Andes-Amazon elevation transect. *Geochim. Cosmochim. Acta* **242**, 64–81.

Fick S. E. and Hijmans R. J. (2017) WorldClim 2: new 1-km spatial resolution climate surfaces for global land areas. *Int. J. Climatol.* **37**(12), 4302–4315.

Freeman K. H. and Colarusso L. A. (2001) Molecular and isotopic records of C_4 grassland expansion in the late Miocene. *Geochim. Cosmochim. Acta* **65**, 1439–1454.

Friedli H., Lotscher H., Oeschger H., Siegenthaler U. and Stauffer B. (1986) Ice core record of the C-13/C-12 ratio of atmospheric CO_2 in the past 2 Centuries. *Nature* **324**, 237–238.

Garcin Y., Schefuß E., Schwab V. F., Garreta V., Gleixner G., Vincens A., Todou G., Séné O., Onana J.-M., Achoundong G. and Sachse D. (2014) Reconstructing C_3 and C_4 vegetation cover using *n*-alkane carbon isotope ratios in recent lake sediments from Cameroon, Western Central Africa. *Geochim. Cosmochim. Acta* **142**, 482–500.

Gillson L. (2004) Testing non-equilibrium theories in savannas: 1400 years of vegetation change in Tsavo National Park, Kenya. *Eco. Complexity*, 281–298.

Gocke M., Kuzyakov Y. and Wiesenberg G. L. B. (2013) Differentiation of plant derived organic matter in soil, loess and rhizoliths based on *n*-alkane molecular proxies. *Biogeochemistry* **112**(1-3), 23–40.

Gocke M., Peth S. and Wiesenberg G. L. B. (2014) Lateral and depth variation of loess organic matter overprint related to rhizoliths - Revealed by lipid molecular proxies and X-ray tomography. *Catena* **112**, 72–85.

Häggi C., Zech R., McIntyre C., Zech M. and Eglinton T. I. (2014) On the stratigraphic integrity of leaf-wax biomarkers in loess paleosols. *Biogeosciences* **11**(9), 2455–2463.

Hargreaves G. L., Hargreaves G. H. and Riley J. P. (1985) Irrigation water requirements for Senegal River Basin. *J. Irrig. Drain. Div.* **111**, 265–275.

Higgins S. I. and Scheiter S. (2012) Atmospheric CO_2 forces abrupt vegetation shifts locally, but not globally. *Nature* **488**(7410), 209–212.

Keeling C., Piper S., Bacastow R., Wahlen M., Whorf T., Heimann M. and Meijer H. (2001) *Exchanges of atmospheric CO_2 and $^{13}CO_2$ with the terrestrial biosphere and oceans from 1978 to 2000. I. Global aspects* SIO Reference Series, No. 01-06. Scripps Institution of Oceanography, San Diego, p. 88.

Krull E. S., Sachse D., Mugler I., Thiele A. and Gleixner G. (2006) Compound-specific $\delta^{13}C$ and $\delta^{2}H$ analyses of plant and soil organic matter: a preliminary assessment of the effects of vegetation change on ecosystem hydrology. *Soil Biol. Biochem.* **38**, 3211–3221.

Krull E. S., Skjemstad J. O., Burrows W. H., Bray S. G., Wynn J. G., Bol R., Spouncer L. and Harms B. (2005) Recent vegetation changes in central Queensland, Australia: evidence from $\delta^{13}C$ and ^{14}C analyses of soil organic matter. *Geoderma* **126**(3-4), 241–259.

Levin N. E., Brown F. H., Behrensmeyer A. K., Bobe R. and Cerling T. E. (2011) Paleosol carbonates from the Omo Group: Isotopic records of local and regional environmental change in East Africa. *Palaeogeog. Palaeoclim. Palaeoecol.* **307**(1-4), 75–89.

Levin N., Quade J., Simpson S., Semaw S. and Rogers M. (2004) Isotopic evidence for Plio-Pleistocene environmental change at Gona, Ethiopia. *Earth Planet. Sci. Lett.* **219**, 93–110.

Lupien R. L., Russell J. M., Feibel C., Beck C., Castañeda I., Deino A. and Cohen A. S. (2018) A leaf wax biomarker record of early Pleistocene hydroclimate from West Turkana, Kenya. *Quat. Sci. Rev.* **186**, 225–235.

Magill C. R., Ashley G. M. and Freeman K. H. (2013) Ecosystem variability and early human habitats in eastern Africa. *Proc. Natl. Acad. U.S.A.* **110**, 1167–1174.

Magill C. R., Eglinton G. and Eglinton T. I. (2019) Isotopic variance among plant lipid homologues correlates with biodiversity patterns of their source communities. *Plos One* **14** e0212211.

Norton-Griffiths M., Herlocker D. and Pennycuick L. (1975) The patterns of rainfall in the Serengeti Ecosystem, Tanzania. *East Afr. Wildl. J.* **13**, 347–374.

Polissar P. J., Rose C., Uno K. T., Phelps S. R. and deMenocal P. (2019) Synchronous rise of African C4 ecosystems 10 million years ago in the absence of aridification. *Nat. Geosci*, 657–660.

Polissar P. J., Uno K. T., Phelps S. R., Karp A. T., Freeman K. H. and Pensky J. L. (2021) Hydrologic Changes Drove the Late Miocene Expansion of C4 Grasslands on the Northern Indian Subcontinent. *Paleoceanogr. Paleoclimatol.* **36**, e2020PA004108.

Quade J., Cerling T. E. and Bowman J. R. (1989) Systematic variations in the carbon and oxygen isotopic composition of pedogenic carbonate along elevation transects in the southern Great Basin, United States. *Geol. Soc. Am. Bull.* **101**, 464–475.

Reed D. N., Anderson T. M., Dempewolf J., Metzger K. and Serneels S. (2009) The spatial distribution of vegetation types in the Serengeti ecosystem: the influence of rainfall and topographic relief on vegetation patch characteristics. *J. Biogeogr.* **36**, 770–782.

Retallack G. (1991) Untangling the effects of burial alteration and ancient soil formation. *Annu. Rev. Earth Planet. Sci.* **19**, 183–206.

Rieley G., Collier R. J., Jones D. M., Eglinton G., Eakin P. A. and Fallick A. E. (1991) Sources of sedimentary lipids deduced from stable carbon-isotope analyses of individual compounds. *Nature* **352**(6334), 425–427.

Rieley G., Collister J. W., Stern B. and Eglinton G. (1993) Gas chromatography/isotope ratio mass spectrometry of leaf wax n-alkanes from plants of differing carbon dioxide metabolisms. *Rapid Commun. Mass Spectrom.* **7**, 488–491.

Rommerskirchen F, Eglinton G, Dupont L, Gunter U, Wenzel C and Rullkotter J (2003) A north to south transect of Holocene southeast Atlantic continental margin sediments: Relationships between aerosol transport and compound-specific d13C land plant biomarker and pollen records. *Geochem. Geophys. Geosyst.* **4**, 1–29.

Rommerskirchen F., Eglinton G., Dupont L. and Rullkötter J. (2006a) Glacial/interglacial changes in southern Africa: compound-specific $\delta^{13}C$ land plant biomarker and pollen records from southeast Atlantic continental margin sediments. *Geochem., Geophys.* **7**. doi.10.1029/2005GC001223.

Rommerskirchen F., Plader A., Eglinton G., Chikaraishi Y. and Rullkötter J. (2006b) Chemotaxonomic significance of distribution and stable carbon isotopic composition of long-chain alkanes and alkan-1-ols in C_4 grass waxes. *Org. Geochem.* **37** (10), 1303–1332.

Sarangi V., Agrawal S. and Sanyal P. (2021) The disparity in the abundance of C_4 plants estimated using the carbon isotopic composition of paleosol components. *Palaeogeog., Palaeoclim., Palaeoecol.* **561**, 110068.

Saylor B. Z., Gibert L., Deino A., Alene M., Levin N. E., Melillo S. M., Peaple M. D., Feakins S. J., Bourel B., Barboni D., Novello A., Sylvestre F., Mertzman S. A. and Haile-Selassie Y. (2019) Age and context of mid-Pliocene hominin cranium from Woranso-Mille, Ethiopia. *Nature* **573**(7773), 220–224.

Schefuss E. and Dupont L. M. (2020) Multiple drivers of Miocene C4 ecosystem expansions.. *Nat. Geosci.* **13**, 463–464.

Schefuss E., Ratmeyer V., Stuut J. B. W., Jansen J. H. F. and Damste J. S. S. (2003) Carbon isotope analyses of *n*-alkanes in dust from the lower atmosphere over the central eastern Atlantic. *Geochim. Cosmochim. Acta* **67**, 1757–1767.

Schmidt M. W. I., Torn M. S., Abiven S., Dittmar T., Guggenberger G., Janssens I. A., Kleber M., Kögel-Knabner I., Lehmann J., Manning D. A. C., Nannipieri P., Rasse D. P., Weiner S. and Trumbore S. E. (2011) Persistence of soil organic matter as an ecosystem property. *Nature* **478**(7367), 49–56.

Schubert B. A. and Jahren A. H. (2012) The effect of atmospheric CO_2 concentration on carbon isotope fractionation in C_3 land plants. *Geochim. Cosmochim. Acta* **96**, 29–43.

Schwab V. F., Garcin Y., Sachse D., Todou G., Séné O., Onana J.-M., Achoundong G. and Gleixner G. (2015) Effect of aridity on $\delta^{13}C$ and δD values of C_3 plant- and C_4 graminoid-derived leaf wax lipids from soils along an environmental gradient in Cameroon (Western Central Africa). *Org. Geochem.* **78**, 99–109.

Sinninghe Damsté J. S., Kuypers M. M. M., Schouten S., Schulte S. and Rullkötter J. (2003) The lycopane/C31 *n*-alkane ratio as a proxy to assess palaeoxicity during sediment deposition. *Earth Planet. Sci. Lett.* **209**, 215–226.

Staver A. C., Archibald S. and Levin S. A. (2011) The Global Extent and Determinants of Savanna and Forest as Alternative Biome States. *Science*, 230–232.

Stevens N., Lehmann C. E. R., Murphy B. P. and Durigan G. (2017) Savanna woody encroachment is widespread across three continents. *Glob. Change Biol.* **23**(1), 235–244.

Targulian V. O. and Krasilnikov P. V. (2007) Soil system and pedogenic processes: Self-organization, time scales, and environmental significance. *Catena* **71**(3), 373–381.

Uno K. T., Polissar P. J., Kahle E., Feibel C., Harmand S., Roche H. and deMenocal P. B. (2016a) A Pleistocene palaeovegetation record from plant wax biomarkers from the Nachukui Forma-

tion, West Turkana, Kenya. *Phil. Trans. Royal Soc. B.* **371** (1698), 20150235. doi.10.1098/rstb.2015.0235.

Uno K. T., Polissar P. J., Jackson K. E. and deMenocal P. B. (2016b) Neogene biomarker record of vegetation change in eastern Africa. *Proc. Natl. Acad. Sci. U.S.A.* **113**(23), 6355–6363.

Vogts A, Moossen H, Rommerskirchen F and Rullkotter J (2009) Distribution patterns and stable carbon isotopic composition of alkanes and alkan-1-ols from plant waxes of African rain forest and savanna C-3 species. *Org. Geochem.* **40**, 1037–1054.

Wang Y. V., Larsen T., Leduc G., Andersen N., Blanz T. and Schneider R. R. (2013) What does leaf wax δD from a mixed C_3/C_4 vegetation region tell us? *Geochim. Cosmochim. Acta* **111**, 128–139.

Wiesenberg G., Schwarzbauer J., Schmidt M. and Schwark L. (2004) Source and turnover of organic matter in agricultural soils derived from n-alkane/n-carboxylic acid compositions and C-isotope signatures. *Org. Geochem.* **35**(11-12), 1371–1393.

Wu M. S., West A. J. and Feakins S. J. (2019) Tropical soil profiles reveal the fate of plant wax biomarkers during soil storage. *Org. Geochem.* **128**, 1–15.

Wynn J. G. (2004) Influence of Plio-Pleistocene aridification on human evolution: evidence from paleosols of the Turkana Basin, Kenya. *Am. J. Phys. Anthropol.* **123**(2), 106–118.

Wynn J. G. (2007) Carbon isotope fractionation during decomposition of organic matter in soils and paleosols: Implications for paleoecological interpretations of paleosols. *Palaeogeog. Palaeoclim. Palaeoecol.* **251**(3-4), 437–448.

Wynn J. G., Bird M. I. and Wong V. N. L. (2005) Rayleigh distillation and the depth profile of $^{13}C/^{12}C$ ratios of soil organic carbon from soils of disparate texture in Iron Range National Park, Far North Queensland, Australia. *Geochim. Cosmochim. Acta* **69**, 1961–1973.

Zomer R. J., Trabucco A., Bossio D. A. and Verchot L. V. (2008) Climate change mitigation: a spatial analysis of global land suitability for clean development mechanism afforestation and reforestation. *Agric. Ecosyst. Environ.* **126**(1-2), 67–80.

Zomer R. J., Trabucco A., Van Straaten O. and Bossio D. A. (2007) Carbon, Land and Water: A Global Analysis of the Hydrologic Dimensions of Climate Change Mitigation through Afforestation/Reforestation, Vol. 101. International Water Management Institute, International Water Management Institute Research Report.

Associate editor: Thomas Wagner